Influence of modifications of HCLL blanket design on MHD pressure losses

C. Mistrangelo *, L. Bühler, C. Koehly, H.-J. Brinkmann

Karlsruhe Institute of Technology, Postfach 3640, 76021 Karlsruhe, Germany

HIGHLIGHTS

- Liquid metal experiments to assess the influence of modifications of HCLL blanket design on MHD pressure drop.
- The test section used for previous experiments has been modified to account for the new design at the first wall.
- Experimental results show that design changes lead to an increase of pressure drop near the first wall by a factor of 3–3.5.
- The influence of 3D MHD phenomena that occur at the FW are more relevant for moderate magnetic fields.

ABSTRACT

In 2008–2009 experiments have been performed to investigate liquid metal magnetohydrodynamic (MHD) flows in a scaled mock-up of a helium cooled lead lithium (HCLL) blanket. In order to improve the mechanical stiffness of HCLL blanket modules the design of the stiffening plate between two hydraulically connected breeder units (BUs) has been later modified. In the former design the liquid metal passed from one BU into the adjacent one by flowing through a narrow gap that extended along the entire width of the BU. In the most recent design this opening has been replaced by a series of smaller gaps. Therefore the velocity increases locally owing to the reduced cross-section along the flow path and the liquid metal contracts and expands along magnetic field lines to enter the neighboring BU. These flow conditions are known to create additional MHD pressure losses. In order to estimate the influence of design changes on MHD flow and pressure drop the previous test section has been adapted to the new design. Experimental results show that the modifications of the design at the first wall lead to an increase of pressure drop near the first wall by a factor 3–3.5. As a consequence the total pressure drop becomes larger. The 3D MHD phenomena that occur at the first wall seem to be mainly related to inertia effects that are confined in layers parallel to the magnetic field.

1. Introduction

The study of liquid metal flows in strong magnetic fields plays an essential role in the development of nuclear fusion reactors where breeding of tritium and heat extraction can be accomplished by circulating in the blanket a lithium-containing alloy. In the Helium Cooled Lead Lithium (HCLL) blanket concept, which will be tested in ITER and possibly employed in a DEMO reactor, the eutectic alloy PbLi is used as breeder material and the heat is removed by helium flowing inside channels embedded in the walls. In the breeder zones the liquid metal flows at low velocity (<1 mm/s) as needed to circulate the PbLi towards external ancillary systems for tritium removal and purification. The HCLL blanket is based on a modular design, where a number of Breeder Units (BU) is arranged in columns to form a module. The box is internally stiffened by a grid of plates to withstand the high helium pressure in case of an accidental in-box leak of coolant. This frame creates an array of rectangular cells where breeding units are positioned.

The complexity of the overall blanket system involves several phenomena, whose global interaction is presently not predictable by numerical or analytical analyses. Therefore experimental investigations are required. Such phenomena are related for instance to electrical coupling of hydraulically separated fluid domains, caused by leakage currents that flow from one fluid domain into the adjacent one by crossing common electrically conducting walls [1]. 3D MHD effects, related to the induction of complex electric current loops, occur due to changes of cross-section along
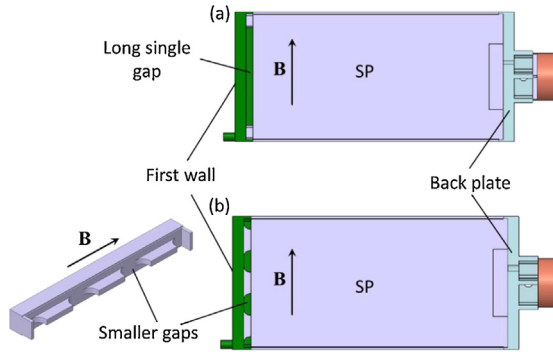
Fig. 1. (a) Original design of the stiffening plate (SP) between two hydraulically connected BUs: top view showing the opening that extends along the total width of the BU. (b) Modified design of the SP at the first wall: the liquid metal flow path consists of a series of small openings.

the flow path, non-uniform magnetic field, and varying electrical conductance of the walls [2,3].

In 2008–2009 an experimental campaign was carried out to study MHD flows in a scaled mock-up of a HCLL blanket according to a design developed at CEA [4], where BUs were connected at the first wall (FW) through a slot that extended over the entire toroidal size of the BU. Results showed that the major pressure drop occurs in manifolds and at the first wall, where the liquid metal passes through the narrow opening connecting two adjacent BUs [5].

In order to improve the structural stability of the HCLL blanket module the design of the stiffening plate between two hydraulically connected BUs was modified [6]. The single large gap in the previous design (Fig. 1(a)) has been substituted by smaller openings (Fig. 1(b)). From an MHD point of view the resulting flow distribution is expected to cause additional pressure drop due to the fact that the flow contracts and expands along magnetic field lines [2]. In order to quantify the influence on MHD flows of design modifications described above, the available test section has been adapted to account for the new design features. Experiments have been performed to record pressure distribution in the new mock-up in a wide range of flow parameters and data has been compared with results obtained by using the former test section.

2. Experimental set-up

2.1. Liquid metal system and characteristic flow parameters

The experiments are performed in the MEKKA laboratory at the Karlsruhe Institute of Technology (KIT) [7]. The eutectic sodium-potassium alloy (Na22K78) is used as working fluid. Physical properties at different temperatures, such as density ρ, kinematic viscosity ν, and electric conductivity σ, are listed in Table 1 according to [8]. Due to the high affinity of alkali metals to oxygen they can react vehemently with air and water. For this reason the liquid metal is permanently stored under an inert gas atmosphere. In the liquid metal loop NaK is circulated by means of a canned motor pump with a maximum pressure head of 0.9 MPa at a flow rate of 25 m³/h for temperatures lower than 150 °C. An electromagnetic pump is used for low flow rates and high temperature runs. The complete liquid metal loop with test section is mounted on a rack

movable on rails by means of a hydraulic piston so that the position of the mock-up can be precisely adjusted inside the magnet. A uniform vertical magnetic field with maximum strength of 2.1 T is provided by a normal conducting dipole magnet. The magnetic gap used for experiments has a rectangular cross-section and within a region of 800 mm × 480 mm × 165 mm the field is pretty uniform with deviations from the core value smaller than 1%.

The dimensionless numbers used to describe the MHD flows studied experimentally are the Hartmann number Ha and the interaction parameter N:

$$Ha = BL\sqrt{\frac{\sigma}{\rho\nu}}, \quad N = \frac{\sigma LB^2}{\rho u_0}. \tag{1}$$

They describe the ratio of electromagnetic to viscous forces and inertia forces, respectively. The Hartmann number serves as non-dimensional measure for the strength B of the imposed magnetic field. The hydrodynamic Reynolds number is related to these quantities as $Re = Ha^2/N$. In (1) L is a typical length scale of the problem corresponding to half of the toroidal size of the mock-up ($L = 0.045$ m), B is the magnitude of the external magnetic field, and u_0 is the average velocity in a cross-section of a breeder unit. In the present experiments we can investigate a broad range of parameters, $500 \leq Ha \leq 5000$, $200 < Re < 10000$. Since NaK has higher electric conductivity σ and smaller density ρ compared to PbLi, it is possible with the laboratory magnetic fields to approach parameter values close to those in fusion applications. With material data for PbLi at 500 °C [9] for a magnetic field $B = 4$ T, a velocity $u_0 = 0.001$ m/s, and full-scale dimension ($L = 0.09$ m) Hartmann and Reynolds numbers in a HCLL blanket are

$$Ha \approx 9200, Re \approx 720. \tag{2}$$

The conductivity of the walls of the test section in comparison with the conductivity of the fluid is expressed through the wall conductance parameter $c = \sigma_w t_w/(\sigma L)$, where t_w is the wall thickness and σ_w the electric conductivity of the wall material, i.e. stainless steel (cf. Table 1 [10]).

2.2. HCLL mock-up and design modifications

The test section manufactured according to the original HCLL blanket design [4] is formed by four BUs connected hydraulically two by two at the first wall through a slot along the entire width of the BU, as shown in Fig. 1(a). A manifold feeds BU1 and BU3 and a second one collects the liquid metal from BU2 and BU4. The flow scheme is depicted in Fig. 2(a). In the modified mock-up the cross-section along the liquid metal flow path from one BU into the adjacent one has been reduced due to the insertion of additional solid parts required to ensure mechanical stiffness. In Fig. 3(b) a picture of the new test section is displayed in which the welding seams are clearly visible at the first wall. In order to integrate the described design modifications [6], the first wall of the former test section has been cut at locations corresponding to the stiffening plates that separate BU1 from BU2, and BU3 from BU4, and new parts have been inserted (Fig. 3(c)).

2.3. Preparation of experiments

After the test section has been modified, a pressure test has been performed to guarantee safe operation during experiments. The test is performed by using pressurized water. The mock-up has been tested successfully up to an internal pressure of 8.6 bar, which permits pressure levels during operation up to 5.6 bar. A leak detection test has been also carried out by using pressurized Argon and by monitoring the pressure level during the day.

Table 1
NaK properties and stainless steel electric conductivity at different temperatures.

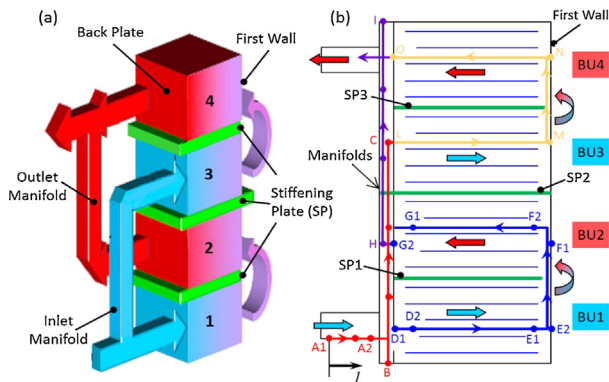| T [°C]	ρ [kg/m³]	ν [10^{-6} m²/s]	σ [$10^6/\Omega$ m]	σ_w [$10^6/\Omega$ m]
20	868.4	1.05	2.88	1.26
40	863.2	0.902	2.79	1.24
60	858.1	0.834	2.70	1.22

Fig. 2. (a) Scheme of liquid metal paths in the test section. The inlet manifold feeds BU1 and BU3 and the second one collects the liquid metal from BU2 and BU4. (b) Dots mark the position of pressure taps and arrows indicate typical flow paths. SP1 and SP3 have a gap near the first wall through which the liquid metal passes from one BU into the adjacent one.

Usually the internal surface of the module is covered by a layer of oxides and impurities that causes a contact resistance between wall and liquid metal. This changes the MHD performance of the test section in comparison with the ideal case when no contact resistance is present [11,12]. For that reason a high-temperature wetting procedure has been performed with the installed mock-up to dissolve into the liquid metal the wall-attached oxide layers. Some fraction of the flow circulates through the purification loop that consists of a cold trap with thermostat. At temperatures above 300 °C a large part of the oxides dissolves in the liquid metal and then precipitates in the cold trap.

2.4. Pressure measurements

Pressure difference between pairs of pressure taps are measured via five capacitive pressure transducers mounted in series. All transducers are sensing the same pressure. The measurement spans of individual transducers overlap to avoid reading errors due to nonlinearity near the end of the ranges. From all five readings the one with the highest accuracy for the considered data is selected as the measured pressure value. For the discussion of the results the dimensional pressure p^* is normalized as $p = p^*/(\sigma u_0 L B^2)$. The pressure distribution is recorded for various Hartmann numbers Ha and interaction parameters N at locations along typical flow paths, marked by different colors in Fig. 2(b). The main contributions to the total pressure drop are identified and results are compared with those obtained in the previous experimental campaign where the original HCLL design was considered [5].

In Fig. 4 pressure is plotted as a function of the coordinate l that varies along the liquid metal flow path (cf. Fig. 2(b)). Results are
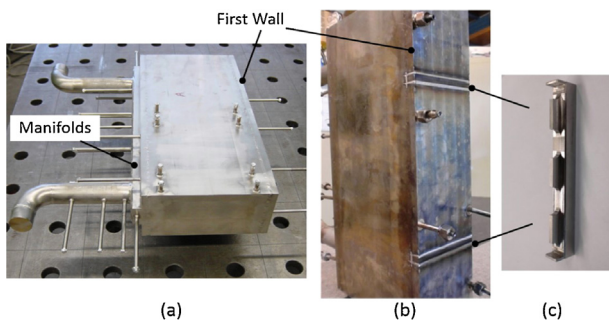

Fig. 3. (a) Manufactured mock-up. (b) View on the first wall of the modified test section. The welding seams indicate the position where the former mock-up has been cut to inserts the new parts shown in (c).
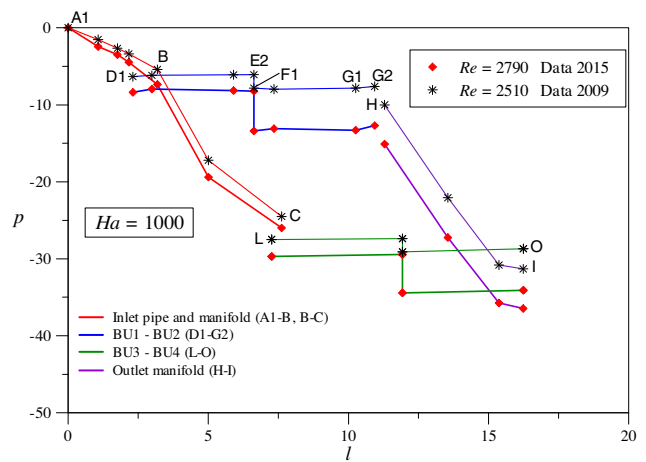

Fig. 4. Pressure distribution along typical flow paths (cf. Fig. 2(b)) for $Ha = 1000$ and a given Reynolds number. The main contributions to the total pressure drop occur along the inlet pipe (A1-B), in the manifolds (B-C, H-I), in the gap at the back plate (B-D1), and across the opening at the first wall (E2-F1). Data obtained in the previous campaign and with the modified test section are compared.

displayed for MHD flow at $Ha = 1000$ and a given Reynolds number. The main contributions to the total pressure drop Δp_{tot} (A1-I) occur in the inlet circular pipe Δp_{in} (A1-B), in the manifolds Δp_M (B-C, H-I), across the gap at the back plate Δp_{BP} (B-D1), and at the first wall Δp_{FW} (E2-F1) [5]. The pressure drop Δp_{BP} results from contraction and expansion of the flow along magnetic field lines from the manifold into the larger BUs. The additional pressure head Δp_{FW} near the first wall, where the liquid metal turns in poloidal direction to enter the connected BU by passing across small openings, is mainly caused by locally larger inertia forces. The latter stem from the increased velocity due to the reduction of the cross-section along the flow path. Inside the breeder units instead the pressure remains almost constant, since the liquid metal flows much slower than in pipes and manifolds. For similar Reynolds numbers the pressure drop at the first wall, Δp_{FW} (E2-F1), is larger when using the mock-up with small openings at the first wall.

Contributions to the total pressure drop that occur in various geometric elements that form the test section are plotted in Fig. 5 as a function of $N^{-1} = Re/Ha^2$ for the flow at $Ha = 1000$. Results obtained with the modified test section (green, solid symbols) are compared with those recorded in the former experimental campaign (red
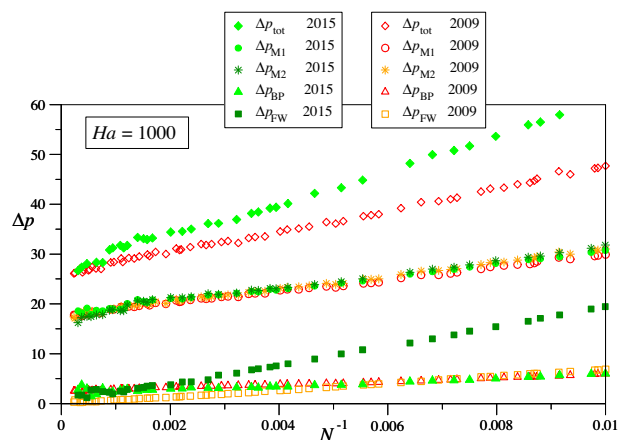

Fig. 5. Contributions to the total pressure drop Δp_{tot}: Δp_{M1} in the distributing manifold, Δp_{BP} across the gap at the back plate, Δp_{FW} through the first wall opening and Δp_{M2} along the draining manifold. Results for $Ha = 1000$. Experimental data obtained during the campaign 2008–2009 are compared with those obtained in 2015 by using the modified test section.
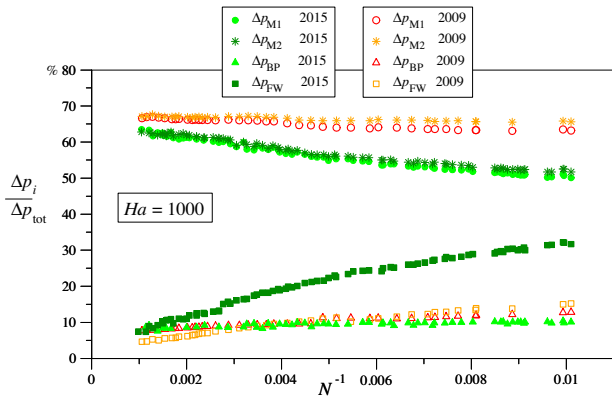
Fig. 6. Main percentage contributions to the total pressure drop Δp_{tot} that occur in manifolds M1 and M2, across the opening in the back plate (BP), and at the first wall (FW) for the flow at $Ha = 1000$. Results from the previous experimental campaign in 2009 are compared with the ones obtained with the modified test section in 2015.
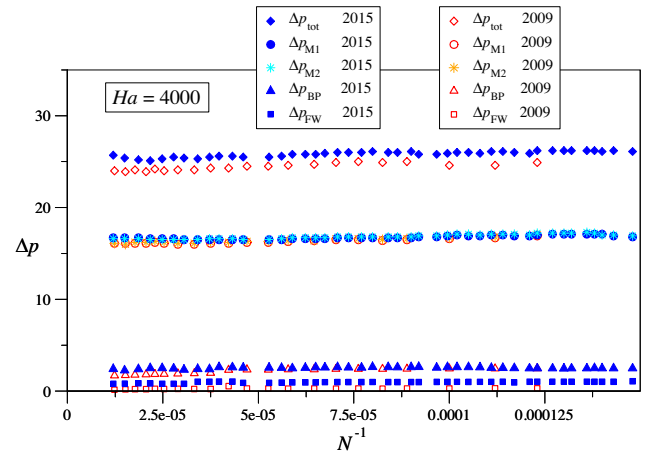

Fig. 7. Main contributions to the total pressure drop Δp_{tot} for the flow at $Ha = 3000$. Results obtained with the modified test section are compared with the ones from the previous experimental campaign (2009).

and orange, open symbols). All pressure contributions vary almost linearly with N^{-1}.

For moderate Hartmann numbers all the contributions depend on the flow rate. However, the pressure drop Δp_{FW} across gaps at the first wall exhibits the most significant dependence on the Reynolds number. It becomes very small for $N^{-1} \rightarrow 0$, suggesting that it is mainly related to the action of inertia forces. Instead, the pressure difference Δp_{BP} across the gap at the back plate, which connects manifold and breeder units, remains rather constant

Fig. 8. Main percentage contributions to the total pressure drop Δp_{tot} that occur in manifolds M1 and M2, across the opening in the back plate (BP), and at the first wall (FW) for the flow at $Ha = 3000$. Data from the experimental campaign in 2009 are compared with the ones obtained with the modified mock-up in 2015.

Fig. 9. Main contributions to the total pressure drop Δp_{tot} for the flow at $Ha = 4000$. Results obtained with the modified test section (2015) are compared with the ones for MHD flows in the original mock-up (2009).
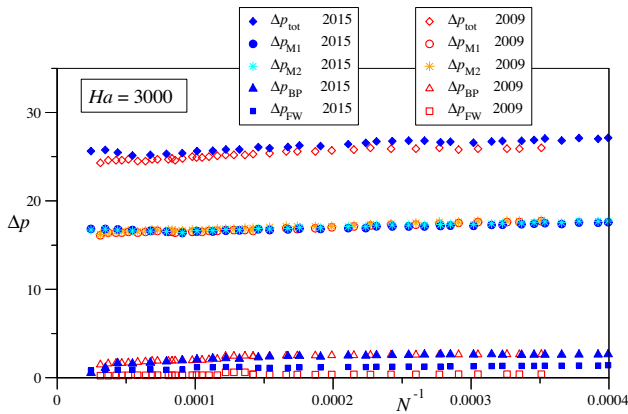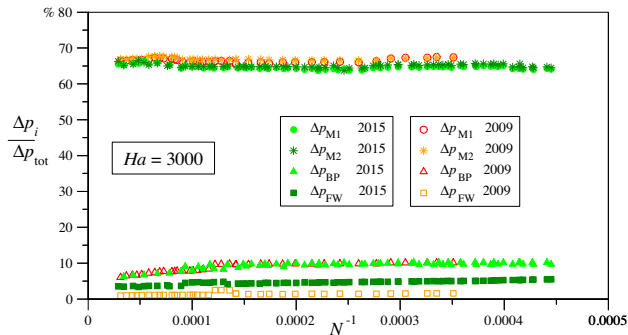
(8–12%) showing that it is determined primarily by electromagnetic phenomena. In Fig. 6 percentage contributions to the total pressure drop are plotted as a function of N^{-1} for the flow at $Ha = 1000$. The main pressure losses occur in manifolds. The pressure heads Δp_{M1} and Δp_{M2} represent about 65% of the total one. Experiments performed with the modified mock-up seem to indicate a stronger dependence of Δp_{M1} and Δp_{M2} on Re compared to previous data. However, their significant percentage reduction for increasing N^{-1} is due to the increase of the total pressure drop owing to the larger contribution of the losses at the first wall, where the liquid metal has to pass through a number of small openings. This is clearly visible in Fig. 6. In the parameter range investigated Δp_{FW} provides 5–35% of the total pressure drop for increasing Re.

For higher applied magnetic field the pressure distribution in the mock-up is nearly unaffected by the flow rate, even for the highest Reynolds numbers that could be reached in the experiments. This can be seen in Figs. 7–9 for MHD flows at $Ha = 3000$ and $Ha = 4000$, respectively. The losses at the FW remain also approximately constant and they provide in the new test section about 5% of the total pressure drop in comparison with 1.5% in the old design. This remaining pressure drop is caused by 3D MHD effects associated with expansion and contraction of the flow along magnetic field lines. Analogously to the results for $Ha = 1000$ discussed above, the total pressure drop increases in the modified mock-up but only of about 4–5%. The impact on the total pressure drop of the 3D MHD effects at the FW becomes smaller for larger Hartmann numbers. Pressure losses in manifolds and at the back plate give a contribution of 65–67% and 8–10%, respectively.

3. Conclusions

The HCLL blanket mock-up used for the experimental campaign 2008–2009 [5] has been modified according to the last review of the design [6]. In the former design at the first wall the liquid metal passed from one BU to the adjacent one by flowing through a narrow gap along the full width of the BU. In the most recent design this slot has been replaced by several smaller openings. Therefore the velocity increases locally owing to the reduced cross-section along the flow path.

Experimental results obtained by using the modified test section show that design changes lead to an increase of pressure drop near the first wall by a factor of 3–3.5. As a consequence the total pressure drop becomes larger too. However, the influence of 3D MHD phenomena that occur at the FW are more relevant for moderate Hartmann numbers ($Ha < 2000$), since they are mainly related to

inertia. For intense magnetic fields the contribution of the pressure drop at the FW is of the order of 4–5%. Therefore, even if these losses slightly increase in the modified design, they are almost negligible compared to pressure drops in manifolds. It can be concluded that, although additional 3D MHD effects actually take place near the FW their influence on the total pressure drop remains rather small especially for strong magnetic fields ($Ha > 2000$). These phenomena seem confined in parallel boundary layers along the first wall. Hence, even if the old design was better from the MHD point of view, the new design is also a possible option, since it only leads to small additional MHD pressure drop compared with other contributions.

Acknowledgments

References

[1] C. Mistrangelo, L. Bühler, Electric flow coupling in the HCLL blanket concept, Fusion Eng. Des. 83 (2008) 1232–1237.

[2] L. Bühler, Three-dimensional liquid metal flows in strong magnetic fields, Technical Report FZKA 7412, Forschungszentrum Karlsruhe, 2008.

[3] O. Andreev, Y. Kolesnikov, A. Thess, Experimental study of liquid metal channel flow under the influence of a non-uniform magnetic field, Phys. Fluids 18 (6) (2006) 065108, Article has been corrected in 2007, vol. 19, 039902.

[4] G. Rampal, A. Li-Puma, Y. Poitevin, E. Rigal, J. Szczepanski, C. Boudot, HCLL TBM for ITER – design studies, Fusion Eng. Des. 75–79 (2005) 917–922.

[5] C. Mistrangelo, L. Bühler, Magnetohydrodynamic pressure drops in geometric elements forming a HCLL blanket mock-up, Fusion Eng. Des. 86 (2011) 2304–2307.

[6] A. LiPuma, G. Aiello, A. Morin, Design description document of the reference option for the HCLL In-TBM breeder unit. Technical Report DEN/DANS/DM2S/SERMA/LPEC/RT/10-4921/A, CEA, 2010.

[7] L. Barleon, K.-J. Mack, R. Stieglitz, The MEKKA-facility a flexible tool to investigate MHD-flow phenomena. Technical Report FZKA 5821, Forschungszentrum Karlsruhe, 1996.

[8] O.J. Foust, Sodium – NaK Engineering Handbook, Gordon and Breach Science Publishers, New York/London/Paris, 1972.

[9] U. Jauch, V. Karcher, B. Schulz, G. Haase, Thermophysical properties in the system Li-Pb. Technical Report KfK 4144, Kernforschungszentrum Karlsruhe, 1986.

[10] Stahl-Eisen-Werkstoffblätter (SEW 310). Physikalische Eigenschaften von Stählen. Verlag Stahleisen Düsseldorf, 1992.

[11] L. Bühler, S. Molokov, Magnetohydrodynamic flows in ducts with insulating coatings, Magnetohydrodynamics 30 (4) (1994) 439–447.

[12] V. Chowdhury, L. Bühler, C. Mistrangelo, Influence of surface oxidation on electric potential measurements in MHD liquid metal flows, Fusion Eng. Des. 89 (7–8) (2014) 1299–1303.